SYSTEM SAFETY: HUMAN - TECHNICAL FACILITY – ENVIRONMENT
7(1), 2025, pp. 443-452

HARDNESS BEHAVIOUR OF SECONDARY A356 ALLOYS: THE INFLUENCE OF IRON AND MANGANESE

DOI: 10.2478/czoto-2025-0041
Received: 10/11/2025
Accepted: 16/12/2025

Zuzana Straková[1] – *orcid id: 0000-0002-4823-2279, e-mail: zuzana.strakova@fstroj.uniza.sk*
Eva Tillová[1] – *orcid id: 0000-0002-1010-0713, e-mail: Eva.Tillova@fstroj.uniza.sk*
Lenka Kuchariková[1] – *orcid id: 0000-0002-2688-1075, e-mail: lenka.kucharikova@fstroj.uniza.sk*
[1] Department of Materials Engineering, University of Žilina, Univerzitná 8215/1 010 26 Žilina, **Slovakia**

Abstract: The rising demand for sustainable materials has led to an increase in the usage of recycled aluminium in the automotive and engineering sectors. However, impurities such as iron, introduced during recycling, can weaken mechanical properties by forming brittle intermetallic phases. This study examines how iron content and manganese addition affect the hardness and microstructure of secondary A356 aluminium alloys. The experimental alloys were produced with Fe levels from 0.080 to 0.586 wt.% and Mn additions up to 0.300 wt.%. Brinell and Vickers microhardness tests were performed to assess overall and local hardness, while microstructure analysis was conducted using scanning microscopy with EDX analysis. Results showed that increasing Fe content slightly raised the hardness due to the formation of Fe-rich Al_5FeSi intermetallic phases, which are brittle and platelet-shaped. The addition of Mn transformed these phases into more compact α-$Al_{15}(Fe,Mn)_3Si_2$ morphologies, improving phase distribution. These findings highlight that controlling Fe content and Mn addition is crucial for optimising the hardness and other mechanical properties of recycled A356 alloys and encouraging the sustainable reuse of aluminium materials.
Keywords: Secondary Aluminium; A356; Brinell; Vickers

1. INTRODUCTION

Aluminium alloy A356 is one of the most widely used Al-Si casting alloys, particularly in the automotive, aerospace and electrical industries, owing to its excellent castability, corrosion resistance, and well-balanced mechanical properties. In recent years, increasing environmental and economic pressures have encouraged industries to replace primary aluminium with secondary (recycled) aluminium, including A356 alloy. Sustainability requirements largely drive this shift, as aluminium recycling requires only about 5% of the energy needed for primary production, resulting in significantly lower production costs and reduced carbon footprint, thereby contributing to global efforts to combat climate change (Reddy and Neeraja, 2018; Vargel, 2020; Raabe et al., 2022).
Despite these advantages, the use of secondary aluminium alloys presents several challenges related to material quality. During the recycling and remelting processes,

various impurities, such as iron, copper, lead or zinc, are introduced into the melt. These impurities originate not only from mixed scrap sources but also from melting equipment and the furnace linings, and are difficult to remove once dissolved. Among them, iron is considered the most detrimental impurity in secondary Al-Si alloys, as it promotes the formation of brittle Fe-rich intermetallic phases, most commonly β-Al_5FeSi (Belov et al., 2002; Burleigh, 2003; Samuel et al., 2023).

These phases typically exhibit a thin, platelet-like morphology that acts as a stress concentrator, leading to reduced ductility, corrosion resistance and fatigue life, and promoting premature crack initiation under cyclic loading (Ji et al., 2013; Ma et al., 2008).

To mitigate the negative influence of iron on microstructure and mechanical properties, manganese is commonly added as a modifying element. Manganese promotes the transformation of brittle platelet-like β-Al_5FeSi phases into less detrimental, more compact α-$Al_{15}(Fe,Mn)_3Si_2$ phase in the Chinese-script or skeleton-like morphology. This morphological modification improves phase distribution and enhances mechanical properties such as hardness and ductility. However, the effectiveness of the manganese addition depends on the Mn/Fe ratio (Dinnis et al., 2005; Pech-Canul et al., 2013; Özyürek et al., 2021).

Recent studies further confirm that the effectiveness of Mn addition strongly depends on the Mn/Fe ratio, with values close to 0.5 being optimal for suppressing the detrimental Fe-rich morphologies and improving mechanical properties in secondary Al-Si alloys. Therefore, this ratio must be carefully controlled to achieve the desired microstructural change (Hwang et al., 2008; Biswas et al., 2021).

Hardness testing remains one of the most effective techniques for evaluating the mechanical behaviour of secondary A356 alloys. The Brinell hardness test provides a general assessment of an alloy's hardness; however, due to the heterogeneous microstructure of recycled aluminium alloys, more localised testing methods are required. The Vickers microhardness test enables the evaluation of hardness in individual microstructural phases, such as aluminium matrix, eutectic silicon, or individual intermetallic phases, allowing a more detailed understanding of structure-property relationships. It should be noted that the morphology, orientation and size of intermetallic phases can significantly influence the measured microhardness values by affecting the material response to indentation (Lan et al., 2019; Biswas et al., 2021).

2. METHODOLOGY OF RESEARCH

2.1. General Background

The research was carried out to examine the influence of iron content and manganese addition on the microstructure and hardness of secondary A356 (AlSi7Mg0.3) aluminium cast alloys. The study aligns with the growing industrial emphasis on recycling aluminium waste for sustainable production – especially in the electric vehicle industry. However, during recycling and melting, impurities such as iron or copper can enter the melt. This results in the deterioration of mechanical and corrosion properties by forming harmful Fe-rich intermetallic phases.

The addition of manganese was found to counter these effects by altering the shape of intermetallic phases, thereby enhancing properties like hardness and corrosion resistance. This study aimed to evaluate these negative effects through metallographic examination and hardness testing.

2.2. Sample of Research

The experimental material used in this study was a secondary aluminium casting alloy A356 (AlSi7Mg0.3), supplied by a Czech manufacturer of aluminium components for the automotive, medical, petrochemical and gas industries. The material was provided as rods with a 20 mm diameter and 300 mm length, produced by gravity casting into sand moulds coated with a protective spray to ensure a high-quality surface. Casting was performed at 750 °C, with melt refining at 740-745 °C using ECOSAL AL 113S.

Five experimental alloys, A, B, B^{Mn}, C and C^{Mn} were cast with varying iron and manganese contents. The chemical composition of experimental alloys is in Table 1. The iron content ranged from 0.080 to 0.530 wt.%, and Mn addition was up to 0.298 wt.%. These chemical compositions were selected to analyse the effect of increased iron content and Mn addition on hardness and microstructure.

Table 1
Chemical composition of experimental samples obtained using Spectrometry [wt.%]

	Si	Mg	Fe	Mn	Ti	Cu	Zn	Al	Mn/Fe
Alloy A	5.782	0.200	0.080	0.005	0.145	0.014	0.049	bal.	0.060
Alloy B	6.032	0.312	**0.382**	0.007	0.136	0.025	0.047	bal.	0.018
Alloy B^{Mn}	6.500	0.261	**0.401**	**0.101**	0.113	0.021	0.051	bal.	**0.251**
Alloy C	6.375	0.314	**0.450**	0.004	0.128	0.009	0.051	bal.	0.008
Alloy C^{Mn}	6.205	0.336	**0.530**	**0.298**	0.127	0.010	0.056	bal.	**0.523**
Balance (bal.) represents the remaining aluminium									

2.3. Instruments and Procedures

Metallographic samples were prepared using standard procedures for Al-Si alloys using the Struers TegraSystem automatic sample preparation unit.

Microstructural analysis was performed using a Zeiss Gemini Sigma 500 scanning electron microscope. This comprehensive analysis included standard microstructural observation, deep-etching analysis, and Energy Dispersive X-ray spectroscopy (EDX).

The hardness of the experimental alloys was determined using Brinell and Vickers hardness tests. The Brinell hardness test was performed on a CV-3000LDB hardness tester following STN EN ISO 6506-1 standard. A carbide ball indenter (Ø 5 mm) and 250 kp test force were applied with a dwell time of 10 s. The Vickers microhardness test was conducted using a Zwick/Roell Micro Vickers hardness tester under a 10 g load for 10 s, following STN EN ISO 6507-1 standard. Both tests were carried out at a minimum of 10 locations on each specimen to ensure statistical reliability. The Vickers test was used to determine the hardness of individual microstructural features, including matrix, eutectic silicon, β-Al_5FeSi and α-$Al_{15}(Fe,Mn)_3Si_2$ intermetallic phases. All tests were performed on samples in the as-cast condition at room temperature.

3. RESULTS AND DISCUSSION

3.1. Microstructural Analysis

The microstructural analysis showed that the main part of the microstructure is the matrix formed by α-phase, accompanied by an eutectic mixture of α-phase and eutectic silicon (Fig. 1). The main intermetallic phases identified in the microstructure were Mg_2Si, Fe-rich intermetallic phases β-Al_5FeSi and α-$Al_{15}(Fe,Mn)_3Si_2$. The Mg_2Si particles are predominantly located near the eutectic silicon and Al_5FeSi phases, appearing as fine, rounded black particles in all tested alloys regardless of the manganese addition.

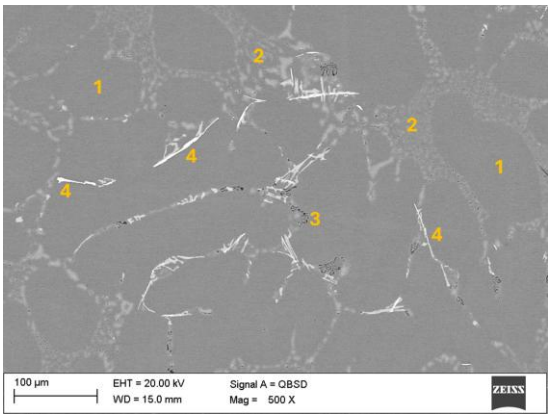

a) Alloy A – 0.080% Fe

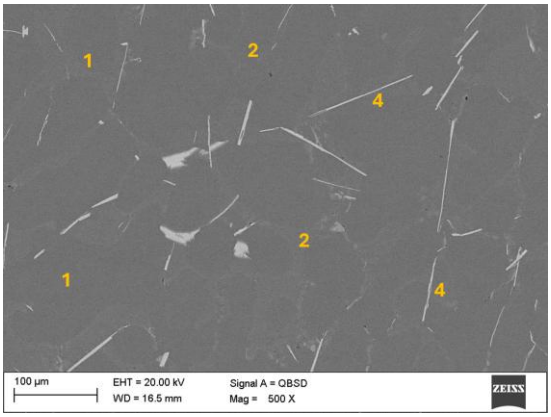

b) Alloy B – 0.382% Fe

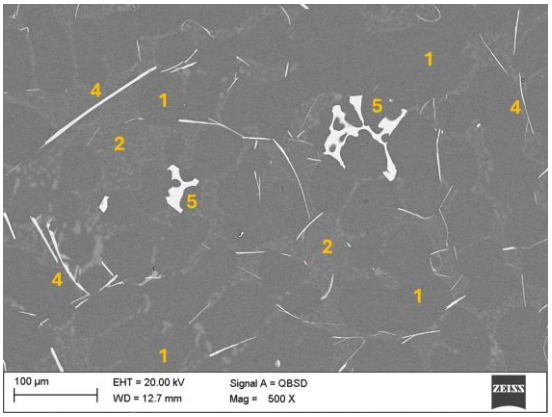

c) Alloy B^{Mn} – 0.401% Fe + 0.101% Mn

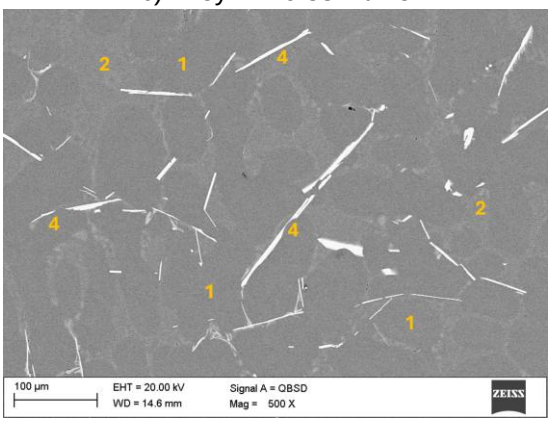

d) Alloy C – 0.450% Fe

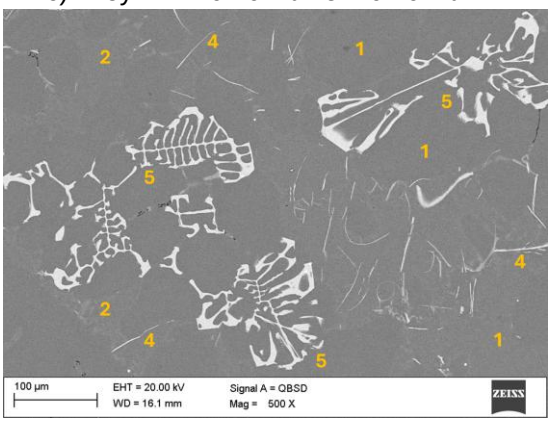

e) Alloy C^{Mn} – 0.568% Fe + 0.298% Mn

Fig. 1. Microstructure of experimental alloys – 1 α-phase; 2-eutectic; 3-Mg_2Si; 4-β-Al_5FeSi; 5-α-$Al_{15}(Fe,Mn)_3Si_2$
SEM, etch. 0.5% HF

The Fe-rich intermetallic phase Al_5FeSi showed a characteristic platelet-like morphology, which became longer and thicker as Fe content increased, and appeared more frequently in the alloys with higher Fe content. To counteract the detrimental effect of iron and Fe-rich intermetallic phases in A356 experimental alloys, manganese was added to change their morphology, provided that an appropriate Mn/Fe ratio of approximately 0.5 is maintained.

The EDX mapping analysis (Fig. 2) shows that aluminium (blue) forms the primary matrix, with silicon (yellow) detected in the intermetallic regions and also as a part of the eutectic

structure, and iron (red) is concentrated in needle-like structures, confirming the formation of the Fe-rich phase. The EDX point analysis (bottom right) quantifies the composition, showing 59.7 wt.% Al, 24.1 wt.% Fe, and 16.2 wt.% Si, confirming the formation of Al_5FeSi. The chemical composition of these intermetallic phases is consistent with the stoichiometry of the β-Al_5FeSi phase. The morphology and the chemical composition identified align with typical features of these phases in A356, confirming their presence in the alloys' microstructure.

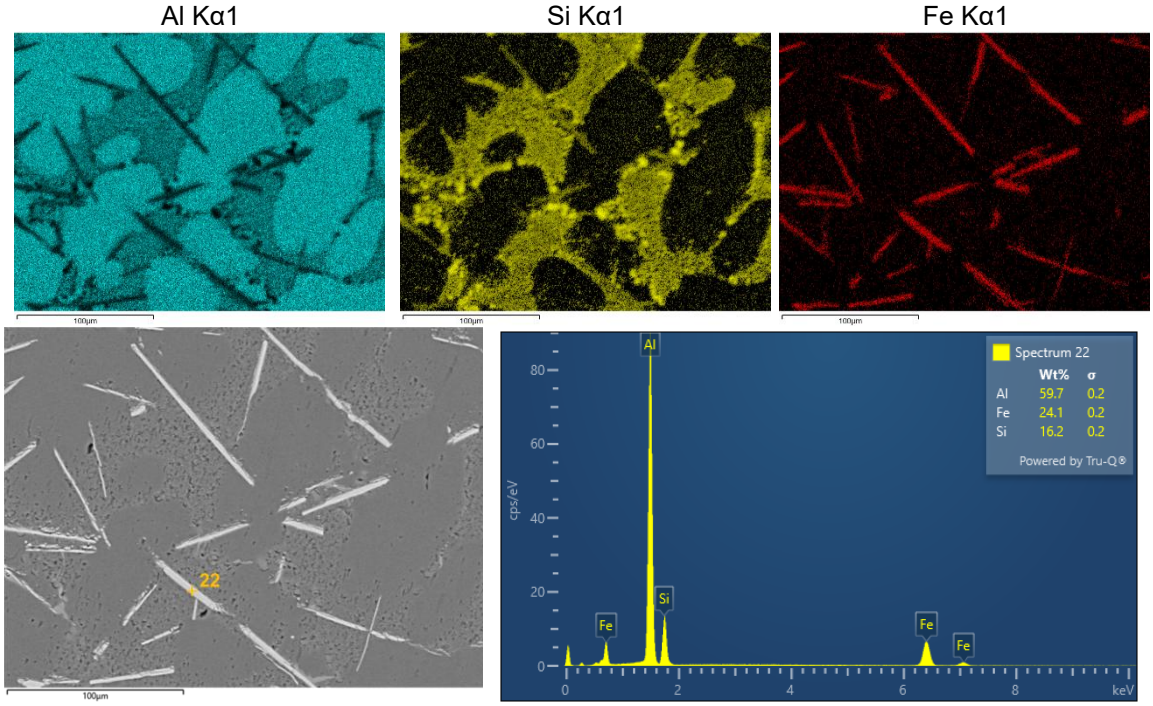

Fig. 2. EDX mapping and point analysis of Al_5FeSi phase, Alloy C, etch. H_2SO_4

The next EDX analysis focused on the $Al_{15}(Fe,Mn)_3Si_2$ intermetallic phase (Fig. 3) in alloys with the addition of manganese (B^{Mn}, C^{Mn}, and D^{Mn}).

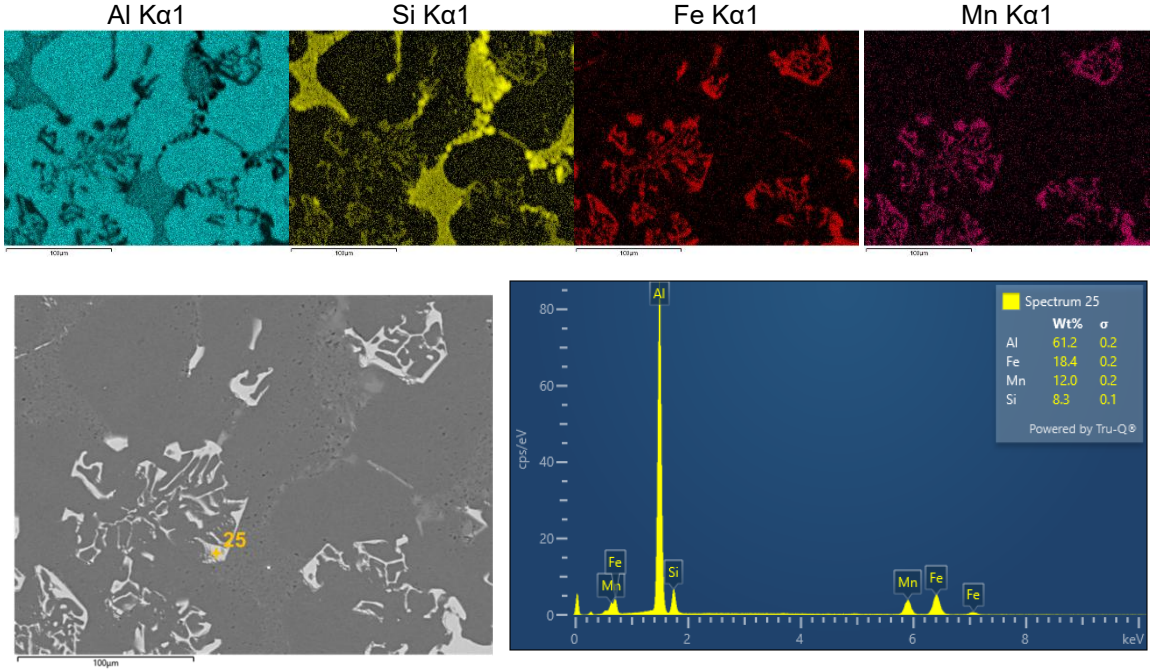

Fig. 3. EDX mapping and point analysis of $Al_{15}(Fe,Mn)_3Si_2$, Alloy C^{Mn}, etch. H_2SO_4

The SEM analysis revealed a Chinese-script-like morphology, distinct from the harmful, needle-like Fe-rich phases, indicating that Mn addition has successfully altered their morphology.

The EDX mapping analysis shows that in addition to aluminium (blue) forming the matrix and silicon (yellow) present in eutectic regions as well as intermetallic phases, iron (red) and manganese (purple) are concentrated in the intermetallic phases, confirming the formation of Fe-Mn-Si phases. The EDX point analysis quantifies the composition, showing 61.2 wt.% Al, 18.4 wt.% Fe, 12.0 wt.% Mn, and 8.3 wt.% Si. The addition of Mn modifies Fe-rich intermetallic phases, reducing the detrimental needle-like morphology and, therefore, should improve alloy properties.

Deep etching was done to significantly improve the visibility of the structural components, enabling a more detailed evaluation of their morphology and spatial distribution. This method selectively dissolved the aluminium matrix while retaining the intermetallic phases, allowing for clearer observation of their three-dimensional characteristics.

Fig. 4a shows the deep-etched Al_5FeSi phase with its characteristic platelet-like morphology, whereas Fig. 4b shows phase $Al_{15}(Fe,Mn)_3Si_2$ with typical skeleton-like morphology.

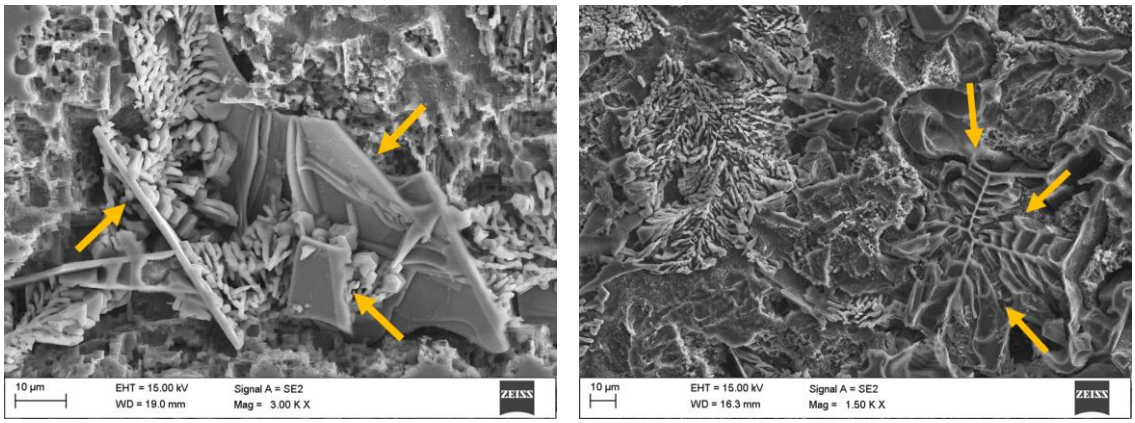

a) b)

Fig. 4. Deep etched a) Al_5FeSi phase and b) $Al_{15}(Fe,Mn)_3Si_2$ phase, SEM, etch. HCl

The Fe-rich intermetallic phases with their platelet-like morphology can act as nucleation sites for eutectic silicon, which appears in a lamellar form, typical of non-heat-treated A356 alloys. This indicates that the eutectic silicon can form adjacent to or directly on the β-Al_5FeSi phase (Shankar et al., 2004; Dahle and Hillert, 2005). The Mg_2Si phase has not been observed in the deep-etched samples, most likely because it was etched off during the etching.

The observed change in Fe-rich intermetallic phases with increasing iron content is consistent with findings reported in previous studies on secondary Al-Si alloys, where higher iron content promotes the formation of elongated β-Al_5FeSi platelets, which have detrimental effects on mechanical properties (Ji et al., 2013; Ma et al., 2008).

The effectiveness of manganese as a modifying element is confirmed by the successful transformation of these Fe-rich intermetallic phases into the α-$Al_{15}(Fe,Mn)_3Si_2$ phases, as reported by Özyürek et al. (2021) and Biswas et al. (2021). These studies both highlight that the appropriate addition of Mn reduces the amount of Fe-rich intermetallic phases and improves the mechanical properties in recycled Al-Si alloys.

3.2. Brinell Hardness Tests

The measured hardness varied depending on the iron content and manganese addition. Alloy A, with the lowest iron content (0.080 wt.%), exhibited the lowest hardness of 50.35 HBW. As expected, the hardness has increased gradually with increasing iron content due to the increasing amount and size of Fe-rich intermetallic phases, which are hard and brittle. Alloy B (0.382 wt.% Fe) reached 57.81 HBW, while Alloy C (0.450 wt.% Fe) exhibited a further increase to 63.46 HBW.

The alloys with manganese addition demonstrated a more complex trend. The manganese addition changed the morphology of the Fe-rich intermetallic phases Al_5FeSi into less harmful phases $Al_{15}(Fe,Mn)_3Si_2$. However, this morphology change does not uniformly increase overall hardness. Alloy B^{Mn} (0.401 wt.% Fe + 0.101 wt.% Mn) exhibited a lower hardness of 55.8 HBW than Alloy B. This could have been caused by failure to achieve the correct Mn/Fe ratio, leading to insufficient morphological change from Al_5FeSi into $Al_{15}(Fe,Mn)_3Si_2$. Alloy C^{Mn} reached the highest hardness value (65.40 HBW), corresponding to an optimal Mn/Fe ratio of 0.5.

The Brinell Hardness values of the experimental A356 alloys are presented in Fig. 5.

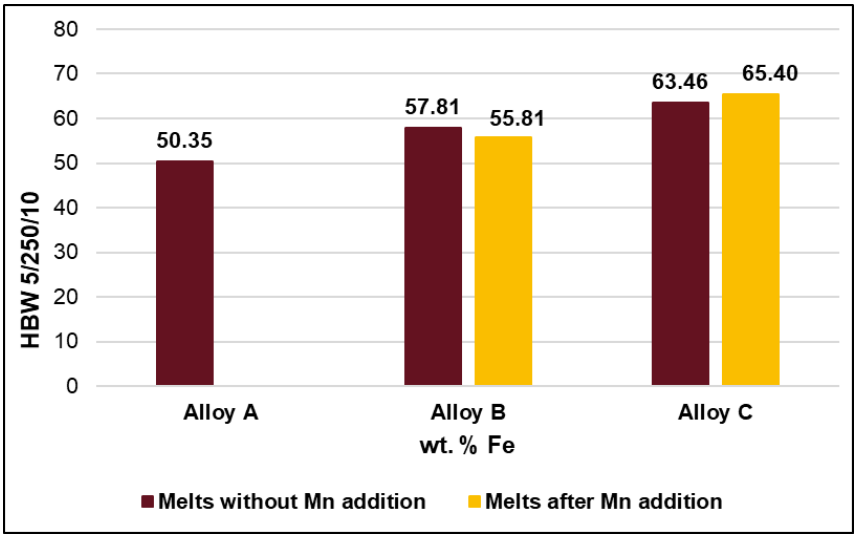

Fig. 5. Brinell hardness test results of experimental samples

The Brinell hardness results reflect the influence of iron content and manganese addition on the microstructure of the A356 alloys. Increasing iron content led to a gradual increase in hardness, primarily due to the higher amount of Fe-rich intermetallic phases, which are harder than the aluminium matrix. The Mn addition modified these phases into less harmful phases, resulting in a more uniform microstructure and hardness, which aligns with the findings of Podprocká et al. (2017).

The effect was the most pronounced in Alloy C^{Mn} with the optimal Mn/Fe ratio and morphological change. Overall, the Brinell hardness test results confirm that controlling Fe and Mn contents and maintaining an appropriate Mn/Fe ratio are crucial for improving the hardness of recycled A356 aluminium alloys. These findings are in agreement with observations by Hwang et al. (2008) and Biswas et al. (2021).

3.3. Vickers Microhardness Tests

This microhardness testing was performed to analyse the hardness of individual microstructural phases in experimental alloys. The aluminium matrix showed an average hardness of 59 HV, as expected for cast A356 alloys. The eutectic regions exhibited an average hardness of approximately 76 HV, reflecting their inherently harder and more brittle character compared to the aluminium matrix. The Mg_2Si particles identified within the microstructure demonstrated an average microhardness of 94 HV. Even though the alloys were not subjected to heat treatment, this value is consistent with the hardness reported in studies by Yildrim (2013) examining the hardness of Mg_2Si after heat treatment.

Table 2
The results of the Vickers microhardness test of individual phases

	Matrix	**Eutectic**	**Mg_2Si**	**Al_5FeSi**	**$Al_{15}(Fe,Mn)_3Si_2$**
HV0.1	59	76	94	779	690

The Fe-rich intermetallic phase – Al_5FeSi, exhibited a notably high average microhardness of approximately 779 HV, although considerable variation was recorded between individual measurements. In certain regions, values exceeded 1000 HV, whereas others were as low as 250 – 400 HV. This variability can be attributed to the anisotropic, platelet-like morphology of the Al_5FeSi phases, which means that the indentations taken on thin edges or less-dense regions register lower values. The exceptionally high hardness values in some places and cracking during measurement confirm the brittle nature of these Fe-rich intermetallics. These findings are consistent with the results reported by Lan et al. (2019), who identified this intermetallic phase as the hardest in the microstructure.
In alloys with manganese addition (B^{Mn} and C^{Mn}), the intermetallic phases containing Mn were also analysed. These $Al_{15}(Fe,Mn)_3Si_2$ phases displayed an even wider hardness range than the Al_5FeSi phases. Some individual measurements reached 1100 HV, while others were as low as 179 HV.
The wide range in microhardness values measured for intermetallic phases is consistent with previous studies, which report strong dependence of local hardness on phase morphology, indentation position and orientation (Lan et al., 2019; Samuel et al., 2023).

4. CONCLUSION

This study evaluated the influence of increasing iron content and manganese addition on the microstructure and hardness of secondary A356 alloys. The main findings are as follows:

- The microstructure of secondary aluminium A356 experimental alloys consists of matrix, eutectic and various intermetallic phases - Mg_2Si, platelet-like Fe-rich Al_5FeSi phase and Chinese-script-like $Al_{15}(Fe,Mn)_3Si_2$ phase.
- Increasing iron content in secondary A356 alloys caused a slight increase in the Brinell hardness, mainly due to the presence of a greater number of Al_5FeSi phase.
- The β-Al_5FeSi phase exhibited brittle platelet-like morphology that can act as a stress concentrator and can reduce the fatigue life of the alloys.
- The addition of manganese changed the morphology of the Al_5FeSi phase into a less detrimental $Al_{15}(Fe,Mn)_3Si_2$ phase in the form of Chinese script.

- The optimal microstructure and hardness were achieved in Alloy C^{Mn}, where the Mn/Fe ratio was closest to 0.5.
- Vickers microhardness confirmed that the intermetallic phases, particularly Al_5FeSi and $Al_{15}(Fe,Mn)_3Si_2$, are significantly harder than the aluminium matrix and eutectic silicon.
- The results demonstrate that precise control of Fe content and Mn/Fe ratio is essential to achieve a balance between the microstructure and mechanical properties of recycled A356 alloys.

ACKNOWLEDGEMENTS

The Ministry of Education, Research, Development and Youth of the Slovak Republic supported the research by projects VEGA 1/0461/24 "Study of a new generation of secondary (recycled) Al-alloys", KEGA no. 009ŽU-4/2023 and KEGA no. 004ŽU-4/2023.

REFERENCES

Belov, N. A., Aksenov, A. A., Eskin, D. G., 2002. *Iron in Aluminium in Alloys*. CRC Press, London, UK.

Biswas, P., Patra, S., Roy, H., Sekhar Tiwary, Ch., Paliwal, M., Mondal, M. K., 2021. *Effect of Mn Addition on the Mechanical Properties of Al–12.6Si Alloy: Role of $Al_{15}(MnFe)_3Si_2$ Intermetallic and Microstructure Modification.* Metals and Materials International, 27, 1713-1727, ISSN 2005-4149, DOI: 10. 1007/s12540-019-00535-5.

Burleigh, T. D., 2003. Corrosion of Aluminum and Its Alloys. Handbook of Aluminum. CRC Press: London, UK.

Dahle, A. K., Hillert, M., 2005. *Discussion of "nucleation mechanism of eutectic phases in aluminum-silicon hypoeutectic alloys*". Metallurgical and Materials Transactions A 36, 1612-1613, DOI: 10.1007/ s11661-005-0253-6.

Dinnis, C. M., Taylor, J. A., Dahle, A. K., 2005. *As-cast morphology of iron-intermetallics in Al–Si foundry alloys.* Scripta Materialia, 53(8), 955-958, DOI: 10.1016/j.scriptamat.2005.06.028.

Hwang, J. Y., Doty, H. W., Kaufman, M. J., 2008. *The effects of Mn additions on the microstructure and mechanical properties of Al–Si–Cu casting alloys.* Materials Science and Engineering: A, 488 (1-2), 496-504, DOI: 10.1016/j.msea.2007.12.026.

Ji, S., Yang, W., Gao, F., Watson, D., Fan, Z., 2013. *Effect of iron on the microstructure and mechanical property of Al–Mg–Si–Mn and Al–Mg–Si diecast alloys.* Materials Science and Engineering: A, 564, 130-139, DOI: 10.1016/j.msea.2012.11.095.

Lan, X., Li, K., Wang, F., Su, Y., Yang, M., Liu, S., Wang, J., Du, Y., 2019. *Preparation of millimeter scale second phase particles in aluminum alloys and determination of their mechanical properties*. Journal of Alloys and Compounds, 784, 68-75, DOI: 10.1016/j.jallcom.2018.12.395.

Ma, Z., Samuel, A. M., Samuel, F. H., Doty, H. W., Valtierra, S., 2008. *A study of tensile properties in Al–Si–Cu and Al–Si–Mg alloys: Effect of β-iron intermetallics and porosity.* Materials Science and Engineering: A, 491 (1-2), 36-51, DOI: 10.1016/j.msea.2008.01.028.

Özyürek, D., Yıldırım, M., Yavuzer, B., Şimşek, İ., Tunçay, T., 2021. *The effect of Ni addition on microstructure and mechanical properties of cast A356 alloy modified with Sr.* Kovove Mater 59, 391-399.

Pech-Canul, M., Giridharagopal, R., Pech-Canul, M. I., Coral, E., 2013. *Localized Corrosion Behavior of Al-Si-Mg Alloys Used for Fabrication of Aluminum Matrix Composites*. Journal of Materials Engineering and Performance, 22(12), 3922-3932, DOI: 10.1007/s11665-013-0674-0.

Podprocká, R., Bolibruchová, D., Chalupová, M., 2017. *Reducing the Negative of the Iron in the Alloy Based on Al-Si-Mg by Manganese.* Archives of Metallurgy and Materials, 17(2), 212-216, DOI: 10.1515/afe-2017-0077.

Raabe, D., Ponge, D., Uggowitzer, P. J., Roscher, M., 2022. *Making sustainable aluminum by recycling scrap: The science of "dirty" alloys*. Progress in Materials Science 128, DOI: 10.1016/j.pmatsci.2022.100947.

Reddy, M. S, Neeraja, D., 2018. *Aluminum residue waste for possible utilisation as material: a review*. Sādhanā, 43(8), 1–8, DOI: 10.1007/s12046-018-0866-2.

Samuel, A. M., Samuel, E., Songmene, V., Samuel, F. H., 2023. *A Review on Porosity Formation in Aluminum-Based Alloys*. Materials, 16(5), 1-26, DOI: 10.3390/ma16052047.

Shankar, S., Riddle, Y. W., Makhlouf, M. M., 2004. *Nucleation mechanism of the eutectic phases in aluminum–silicon hypoeutectic alloys*. Acta Materialia, 52(15), 4447-4460, DOI: 10.1016/j.actamat.2004.05.045.

STN EN ISO 6506-1: 2015 (43 0371), *Kovové materiály. Brinellova skúška tvrdosti.*

STN EN ISO 6507-1: 2024 (42 0374), *Kovové materiály. Vickersova skúška tvrdosti.*

Vargel, C., 2020. *Corrosion of Aluminium*. Elsevier, Amsterdam, Netherlands.

Yildrim, M., Özyürek, D., 2013. *The effects of Mg amount on the microstructure and mechanical properties of Al–Si–Mg alloys*. Materials & Design, 51, 767-774, DOI: 10.1016/j.matdes.2013.04.089.